Spatial and temporal variations in sediment accumulation rates in a freshwater tidal marsh channel of the Patuxent River, Maryland

Kelsey Lynn Wood, Advisors: Karen Prestegaard and Alan J. Kaufman

Background

Sea level in the Chesapeake Bay area has been rising at a rate of 2-4 millimeters a year which raises concern for the survival of tidal marshes. Freshwater tidal marshes are an important part of coastal ecosystems. They act as buffers for storm surges, habitats for aquatic life, and have ample economic value. (Mitsch & Gosselink, 2000) They are vital to the state of water chemistry as they are centers of sediment retention and denitrification (Seldomridge & Prestegaard, 2014). Marshes ability to store nutrients becomes ever more vital to the health of an estuary with an increase of urban and agricultural land use within the basin. The Patuxent watershed has gone from being primarily forested to become >15% urban and >20% agricultural. In order for marshes to adapt, net sediment accumulation should be equal to the local apparent rise in sea level. Many factors affect the accumulation of sediment within a tidal channel network, such as sediment concentrations within the estuary, channel form, water velocities, and the presence of vegetation within the channel.

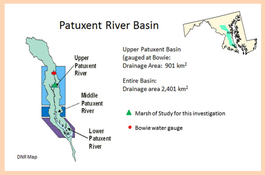

Figure1: Map of the Patuxent River basin. Images modified from Maryland DNR

Figure 2: Marsh on which this study is focused. Upper Marlboro, Maryland. 38°48'05"N and 76°42'20"W

Hypotheses

1. The proportion of mineral sediment to organic sediment will decrease with distance upstream into the tidal channel network.

-Core samples taken near the channel inlet will have the highest mineral sediment content and the highest bulk density.
-Core samples at upstream locations will have the highest organic sediment content and the lowest bulk density.

2. Although sediment type (organic or mineral) will vary spatially, the rate of accumulation is determined by accommodation space rather than sediment availability, and therefore will be similar throughout the tidal channel network. Consequently, the shift in ^{15}N composition observed in Fowler's (2014) cores, will occur at similar depths in cores taken from all locations.

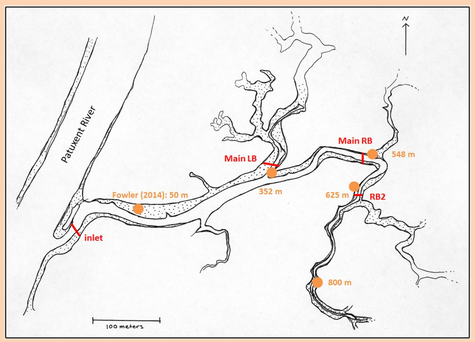

Figure 3: Map showing cross sectional locations used for potential sediment transport calculations and sites of sediment core samples used for bulk density, combustion and isotopic analysis.

Methods and Results

I. Channel morphology measurements

Measurements were made of total channel width, water width, and vegetated width at 20 m intervals along the channels. Measurements for summer conditions were performed on USGS air photos from 8/28/2010.

Results:

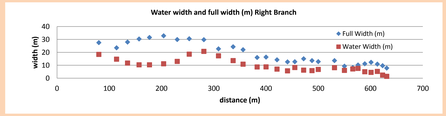

Figure 4:Total channel width and non-vegetated channel width as a function of the distance upstream (main channel and right branch channel).

Six cross sections were measured at permanently anchored sites during high tide. I also acquired data from a cross section near the inlet of the channel that was previously measured by Statkiewicz (2014). Sites for field cross section measurements were selected to provide data for intervals along the main channels and at sites near distributary junctions

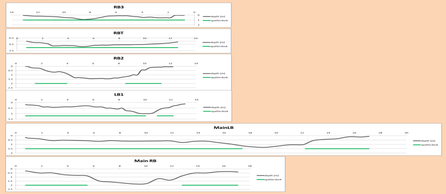

Figure 5: measured cross sections of the tidal marsh channel.

II. Vertical and spatial distributions of suspended sediment by grain size

Theory and Methods: The maximum suspended particle size and its vertical distribution within the water column can be predicted based on channel morphology, and tidal hydrodynamics. Rouse (1937) developed a theory for the vertical distribution of sediment, which is based on the vertical velocity profile in a channel cross section and the fall velocity of the sediment. Suspension occurs when upwards turbulence (the vertical component of velocity) is greater than the fall velocity of the particle, W_s. The shear velocity, u*, is calculated as: $u^* = \sqrt{gdS}$

Where *g* is gravitational acceleration, *d* is flow depth, and *S* is gradient.
The fall velocity can be calculated as:

$$W_s = \frac{RgD^2}{C_1 v + (0.75 C_2 RgD^3)^{(0.5)}}$$

Where *Rg* is the particle Reynolds number, *D* is the grain diameter, *v* is the kinematic viscosity of the matrix which is in this case is water, and C_1 and C_2 are coefficients that depend upon grain size and shape. (Ferguson and Church, 2006).
The vertical distribution of sediment in the water column is calculated using the Rouse equation, where the vertical distribution of sediment of each grain size is governed by the exponent, *Z*: $Z = \frac{W_s}{\beta k u_*}$

Where *b* is assumed to be 1.0, and *k* is Von Karman's constant (0.4).
Rouse's equation to determine the sediment concentration relative to the sediment concentration near the bed, *C/Ca*, for any given depth can be calculated:

$$\frac{C}{C_a} = \left(\frac{d-y}{y} * \frac{a}{d-a}\right)^Z$$

Where *C* is concentration, *d* is total depth, *y* is the distance above the bed, and *a* is an arbitrary distance above the bed used as a reference level (usually taken to be 0.05 of the depth above the bed).

The Rouse calculations of the vertical distribution of sediment of various grains sizes were combined with vertical distribution of velocity measurements recorded during a Spring (high) tide during vegetated conditions by Statkiewicz (2014). For each depth the sediment flux was calculated as the product of concentration and velocity. The depth at which the maximum flux was achieved for each grain size was used to identify the depth and thus flow velocity to use to calculate the maximum transport distances

Results: Rouse calculations showed similar sediment transport potential for the various cross sections. The length of a tidal cycle is the primary limiting factor on transport distance of each grain size. The larger grain sizes are unable to travel great distances into the channel or onto the *Nuphar* bench.

II. Suspended sediment analysis (continued)

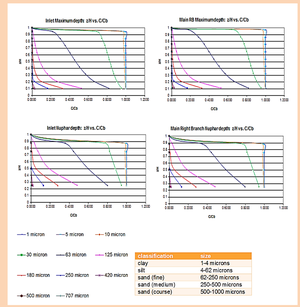

Figure 6: Vertical distributions of suspended sediment concentration by grain size. Vertical relative concentrations were calculated with the Rouse equation for the cross section locations shown in figure 7.

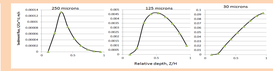

Figure 7: Peak flux calculations for sand and silt-sized particles.

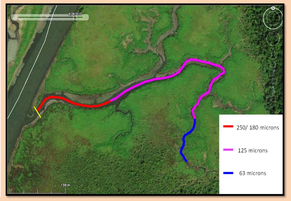

Figure 8: map of maximum potential transport distances during a Spring (high) tidal cycle for the indicated grain sizes. Grain size maximum distances: 250 & 180 microns = 202 meters; 125 microns= 680 meters; 63 microns= 800 meters.

III. Analysis of Sediment Cores

Core preparation and bulk density determination

Sediment cores were cut into 2.5 cm increments, dried, and weighed to calculate bulk density:

$$\rho = \frac{mass}{volume}\left(\frac{g}{cm^3}\right)$$

Combustion of organic matter

The homogenized sediment samples are weighed into 1g aliquots and placed in a kiln heated to 450ºC for 10 hours. This will cause all the organic matter to ignite and combust, creating carbon dioxide. After combustion the samples are weighed again to determine the mass lost to organic matter.

Results:

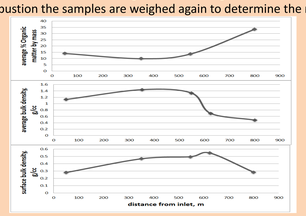

Figure 9: average percent organic matter by mass and bulk density as a function of distance each core was retrieved from the inlet to the tidal channel network.

Carbon and nitrogen elemental and isotopic analyses

The isotope analysis was performed in a stable isotopes laboratory using **a *Euro EA Elemental Analyzer*** and an ***Isoprime isotope ratio mass spectrometer*** with the guidance of lab manager Rebecca E. Plummer.

Each sample, contained in its tin capsule, is loaded into the *Euro EA Elemental Analyzer. Each sample is* dropped into a combustion/ oxidation column heated to 1040ºC. A gas chromatograph separates the nitrogen gas (N_2) or the carbon dioxide (CO_2) from the remaining gasses. They are then transported to the *Isoprime isotope ratio mass spectrometer.* Here they are ionized and steered by an electromagnet to separate Faraday cup receptors. All samples were measured against lab standard tanks of CO_2 and N_2; nitrogen was standardized according to *VPDB*, and carbon was standardized according to *V-air*.

Results:

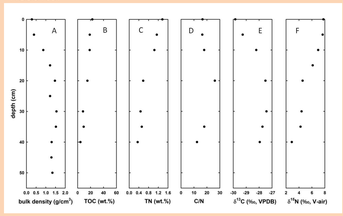

Figure 10: Core closest to the inlet, isotope analysis from (Fowler, 2014). A: core sediment bulk density (g/cc). B: Total organic carbon (weight %). C: Total nitrogen (weight %). D: Carbon to nitrogen ratio (C/N). E: ^{13}C elemental composition (ppm, VPDB). F: ^{15}N elemental composition (ppm, V-air).

III. Core analysis (continued)

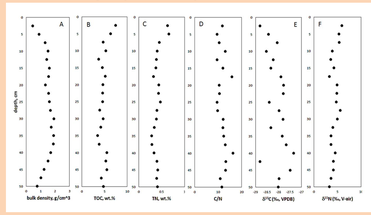

Figure 11: Intermediate distance from the inlet retrieved 352 meters from the inlet. Error: N=±0.13ppm, C=±0.06ppm. A: core sediment bulk density (g/cc). B: Total organic carbon (weight %). C: Total nitrogen (weight %). D: Carbon to nitrogen ratio (C/N). E: ^{13}C elemental composition (ppm, VPDB). F: ^{15}N elemental composition (ppm, V-air).

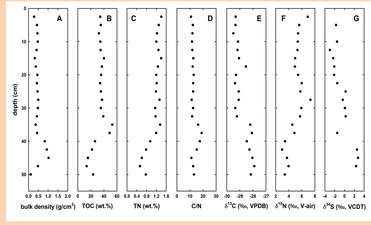

Figure12: Core furthest from the inlet. Error N= ±0.13 ppm, C= ±0.04ppm. A: core sediment bulk density (g/cc). B: Total organic carbon (weight %). C: Total nitrogen (weight %). D: Carbon to nitrogen ratio (C/N). E: ^{13}C elemental composition (ppm, VPDB). F: ^{15}N elemental composition (ppm, V-air). G: ^{34}S analyses performed by Dr. Alan Jay Kaufman.

Conclusions and Discussion

1. These data indicate a decrease in bulk density and an increase in organic matter with distance upstream into the marsh. These data are consistent with hypothesis 1.
2. The initial rise in $\delta^{15}N$ was found at similar depths in the inlet core (Fowler, 2014) and the intermediate core at 352 meters. The $\delta^{15}N$ shift in the upper core was found at a great depth. The top 25 cm of the upper marsh core appears relatively homogeneous, which was also unlike the other two cores. Therefore, hypothesis 2 was not supported.

Discussion

The upper portion of the organic-rich core has a low bulk density and this material may be easily eroded in winter when it is not protected by submerged aquatic vegetation. Accumulation during summer months could account for this upper homogeneous layer and the greater depth to the $\delta^{15}N$ shift (Fig. 13).

Accumulation history

There is a significant decrease in mineral sediment beginning at about 20 cm depth in both the inlet and the intermediate core. The Brighton Dam of the Patuxent River, built in 1943, has decreased sediment fluxes . If this peak at 20 cm is assumed to be 1943, then the average accumulation rate would be 2.7 mm a year, which would match the average sea level rise rate.

Based on these observations and the observations of Statkiewicz (2014), it would appear as though this tidal marsh channel is adequately adapting to the current sea level rise rate.

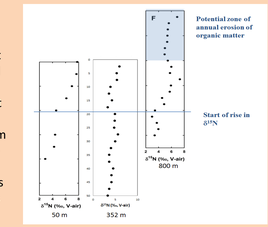

Figure 13: spatial comparison of temporal estimations based on $\delta^{15}N$ values.

References

Ferguson, R. I., and M. Church (2006), *A Simple Universal Equation for Grain Settling Velocity*, Journal of Sedimentary Research, 74(6) 933-937

Fowler, E. (2014). *Carbon and Nitrogen Abundance, Isotope Fractionation, and Aquatic vegitation decay rates in Patuxent Freshwater Wetlands.*

Mitsch, W. J., & Gosselink, J. G. (2000, October). The value of wetlands: importance of scale and landscape setting. *Ecological Economics*, pp. 25-33.

Rouse, H. (1937). Modern Conceptions of the Mechanics of Fluid Turbulence. *Transactions of the American Society of Civil Engineers*, 463-505.

Seldomridge, E., & Prestegaard, K. (2014). Geochemical, Temperature, and Hydrologic Transport Limitations on Nitrate Retention in Tidal Freshwater Wetlands, Patuxent River, Maryland. *Wetlands*, 641-651.

Statkiewicz, A. E. (2014). *Vegitation-hydrodynamic interactionsand the stability of channel inlets in tidal freshwater wetlands, Chesapeake Bay system*